Nat. Hazards Earth Syst. Sci., 9, 1643–1653, 2009
www.nat-hazards-earth-syst-sci.net/9/1643/2009/

Natural Hazards and Earth System Sciences

Identification of potential rockfall source areas at a regional scale using a DEM-based geomorphometric analysis

A. Loye, M. Jaboyedoff, and A. Pedrazzini

Institute of Geomatics and Risk Analysis, University of Lausanne, Lausanne, Switzerland

Received: 30 January 2009 – Revised: 19 August 2009 – Accepted: 25 August 2009 – Published: 8 October 2009

Abstract. The availability of high resolution Digital Elevation Models (DEM) at a regional scale enables the analysis of topography with high levels of detail. Hence, a DEM-based geomorphometric approach becomes more accurate for detecting potential rockfall sources. Potential rockfall source areas are identified according to the slope angle distribution deduced from high resolution DEM crossed with other information extracted from geological and topographic maps in GIS format. The slope angle distribution can be decomposed in several Gaussian distributions that can be considered as characteristic of morphological units: rock cliffs, steep slopes, footslopes and plains. A terrain is considered as potential rockfall sources when their slope angles lie over an angle threshold, which is defined where the Gaussian distribution of the morphological unit "Rock cliffs" become dominant over the one of "Steep slopes". In addition to this analysis, the cliff outcrops indicated by the topographic maps were added. They contain however "flat areas", so that only the slope angles values above the mode of the Gaussian distribution of the morphological unit "Steep slopes" were considered. An application of this method is presented over the entire Canton of Vaud (3200 km^2), Switzerland. The results were compared with rockfall sources observed on the field and orthophotos analysis in order to validate the method. Finally, the influence of the cell size of the DEM is inspected by applying the methodology over six different DEM resolutions.

1 Introduction

Rockfall is defined as individual rocks removed from a slope by sliding, toppling or falling and proceeding downslope (Varnes, 1978). The size of the blocks ranges from small cobbles to large boulders of 100 m^3 (Whalley, 1984). Rockfall risk in mountainous areas is increasing as the population and economic activity increase (Baillifard et al., 2004; Leroi et al., 2005). As a consequence, the identification of rockfall hazard prone areas is of primary importance for producing hazard maps. Several approaches at local and regional scale have been developed to identify rockfall source areas and to assess the resulting hazard or susceptibility (Mazzoccola and Hudson, 1996; Bunce et al., 1997; Guzzetti et al., 1999; Gokceoglu et al., 2000; Jaboyedoff et al., 2005a). During the last two decades, the increasing availability of digital elevation models (DEMs) and GIS data have given rise to a variety of very convenient rockfall models at various scales (Guzzetti et al., 2002; Günther, 2003; Baillifard et al., 2003; Jaboyedoff et al., 2004a; Derron et al., 2005).

However, one of the main difficulties in mapping rockfall hazard at a regional scale is the identification of potential rockfall sources. Those source areas, which correspond to the detachment zones of the blocks, are usually taken from distinctive evidence such as talus slope and scree deposits below cliff faces (Frattini et al., 2008), field and historical inventory of rockfall (Hantz, 2003). Whether these datasets are available, they are often fragmentary in space and time. A variety of empirical, statistical and process-based methods for detecting source areas exists, but only few of them were tested for identifying source zones at a regional scale (>500 km^2) (Crosta and Agliardi, 2003). The simplest morphometric approach consists of defining a thresholds angles above which the slope, especially the rock cliffs, may be considered as unstable (Toppe, 1987) (e.g. >60° in Guzzetti et al., 2003; >45° in Jaboyedoff and Labiouse, 2003; >37° in Frattini et al., 2008). Similar attempts were limited to cliff faces (Krummenacher, 1995; Meissl, 1998) or active rockfall slopes only (van Dijke and van Westen, 1990). More evolved methods were developed by combining the slope geometry extracted from a DEM with datasets such as rock type, exposition, slope curvature and land cover for instance in an heuristic or probabilistic way (Marquinez et al., 2003; Aksoy and Ercanoglu, 2006; Acosta et al., 2007). Besides, high resolution DEMs (HRDEMs) have made possible the detection

Correspondence to: A. Loye
(alexandre.loye@unil.ch)

Published by Copernicus Publications on behalf of the European Geosciences Union.

of discontinuities sets (Jaboyedoff et al., 2007). Considering the spatial arrangement of discontinuities with the topography, a kinematic analysis can then be performed to detect potential failure mechanisms (planar sliding, wedge failure and toppling) (Wagner et al., 1988; Rouiller et al, 1998; Gokceoglu et al., 2000; Jaboyedoff et al., 2004b, 2005b; Günther et al., 2004; Derron et al., 2005). Those geometrical and geomechanical-based approaches are especially suitable for slope stability analyses in well-known regions where rockfall cause problems. They require however local information on the discontinuity sets that can only be partly obtained with automatic procedures on DEM. Therefore, field work is usually required.

According to Heim's studies (Heim, 1932), one of the main factors necessary for rockfall initiation is a steep slope angle. Gravity-driven surface processes in mountainous regions are closely related to the steepness of the topography and the morphology of the relief, which therefore reflects these instabilities (Montgomery and Brandon, 2002). The slope angles of stability depend on the rock type and the geometrical and mechanical properties of the discontinuity sets (Hoek and Bray, 1981; Selby, 1993). This fact includes frictional angle and cohesion when assuming a Mohr-coulomb failure criterion (Locat et al., 2000). Therefore, it can be considered that the slope angle distribution reflects the type of relief (e.g. glacial, alluvial, plains, etc.) and the mechanical properties of the rocks. As a consequence, different morphologies and rock types induce a range of slope angle values that are characteristic for a given morphotectonic setting (Strahler, 1954) and expressed in a slope angle distribution (SAD). As an example (Fig. 1), the SAD of an Alpine valley profile represented by two morphological units varies randomly around their mean slope angles (20° for the footslopes and 60° for the cliffs), implying a Gaussian distribution of the slope angles around these means. As zones with high curvature are less represented, the morphological units (MU) can be extracted according to their slope angle frequency distribution and assuming a Gaussian-shape curve.

Currently, modern acquisition techniques (Airborne Laser Scanning, Photogrammetry) enable to obtain a regional scale DEM with a resolution as high as 1 m making the topographical analysis more and more relevant since the modelled slope angles are very close to reality. For instance (Fig. 2), for a cliff of 20 m high, a 25 m cell size grid gives an apparent slope angle significantly smaller (60°) compared to a HR-DEM grid of 2 m resolution (∼90°). This study introduces a methodology that enables detecting rockfall sources at a regional scale, based on a geomorphometric analysis performed on such HRDEMs (1 m cell size).

2 Methodology

The study area is divided in homogeneous morphometric areas (HMA) following identical characteristics such as uniform lithology, geologic and morphotectonic history. Potential rockfall initiation areas are determined by analysing the SAD of the main HMA. The SAD is decomposed into several Gaussian slope angle distribution characteristics of a specific morphological unit (Strahler, 1950) such as the cliffs, steep slopes, footslopes and plains for an Alpine valley. The Gaussian distribution "cliffs" enables to extract cliff faces, outcropping areas and bare rock surfaces that can be considered as potential rockfall sources. In addition, the detection of rockfall based on the distribution of the slope angle can be improved by using other documents like geological maps, topographic maps and orthophotos.

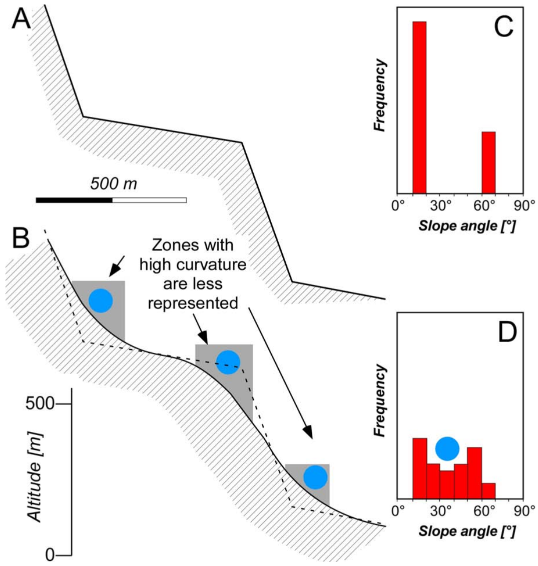

Fig. 1. Ideal sketch profile (A) and realistic profile (B) of an Alpine valley representing two cliffs and two steep slopes; (C/D) their slope angle distribution (SAD) (modified after Rouiller et al., 1998).

2.1 Slope angle distributions (SAD) and its decomposition

The study area is grouped into HMA having similar structural style and morphology as well as close geomechanical behaviour. The underlying assumption states that the slope profiles are different varying HMA. The effective surface area of each grid cell of a DEM depends on its inclination (slope angle), the surface areas of the steep slopes are underestimated in comparison to flat zones (planimetric). In order to consider an effective surface of the topography for the SAD analysis, the 1 m^2 surface of the DEM cells are weighted according to the slope angle β of the HRDEM. The frequency (w_β) of the SAD is then calculated using:

$$w_\beta = \frac{A_{h\beta}}{A_{\mathrm{HMA}} \cos\beta} \qquad (1)$$

where $A_{h\beta}$ is the sum total horizontal area of the DEM cells with the same slope angle β and A_{HMA} is the total area

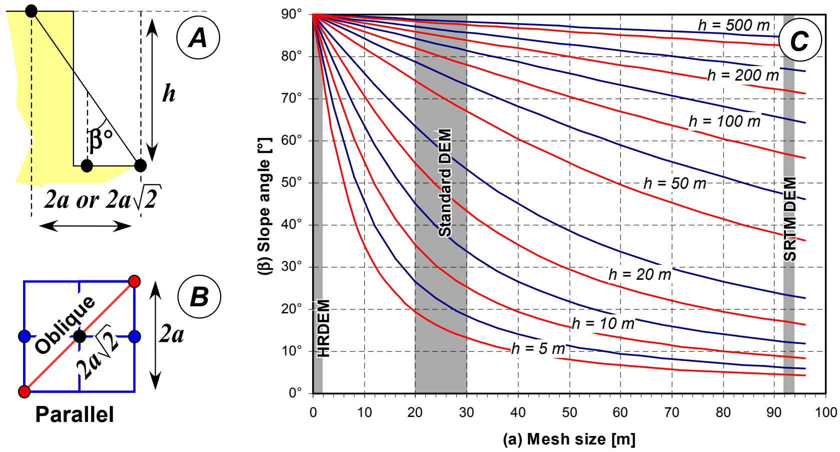

Fig. 2. (A) Relationship between slope angle and cliff height. (B) Computation of the slope angle depending on the orientation of the cliff. (C) Slope angle β computed from a DEM grid of size a for a vertical cliff face of height h. The difference between the red and blue line in (C) indicates the difference between a cliff parallel and oblique (45°) to the DEM grid cells.

of the HMA considered. Then, the obtained SAD can be modelled by Gaussian distributions that can be related to the main morphological units of the topography (Strahler, 1950). Hence, the method consists in decomposing the SAD into several Gaussian (slope angle) distributions characteristic of the main morphological units (GDMU) of a given topography (Fig. 3). The decomposition of the SAD into GDMU is performed by minimizing standard error of the estimated SAD (the sum of the GDMUs) versus computed SAD. In the present study, four main morphological units (MU) can be identified:

1. Plains: low slope angles corresponding to the fluvial and fluvio-glacial deposits.
2. Foot-slopes: gentle slope angles featuring the lower part of the hillslope characterized by colluvial fans, debris flow and landslide deposits.
3. Steep slopes: containing till deposits and rocky outcrops covered with vegetation.
4. Cliffs: very steep slopes, which correspond to rocky outcrops.

The two last morphological units may contain rockfall source areas. They are the units to focus on, in order to define the threshold slope angles above which rockfall sources can be found. The comparison between these MU extracted with Gaussian distribution and the ones on the hillshade shows that they are accurately superimposed (Fig. 4). The above assumptions are however not always verified. As a consequence, a part of interpretation of the GDMU is necessary.

2.2 Method adaptation for non-Alpine topography

This morphological classification can be applied on less rugged landscapes as well. Where large flat zones with small slope angles are dominant, the frequency of slope angles above 30° is very low. This is due to the fact that rugged landscapes are too sparse throughout such a foreland or hilly landscape. The topography is not mirrored in a homogeneous way. Consequently, GDMU extraction is too difficult. Therefore, the GDMU can be calculated based on a SAD coming from a serie of cross-sections along the rugged areas only, without considering any large flat zones in between. Thus, the SAD analysis focuses only on the steep terrain, where rockfall activity is likely to occur. After comparison with the specific test zones, 30 profiles have shown to render the overall slope angle distribution in an accurate way.

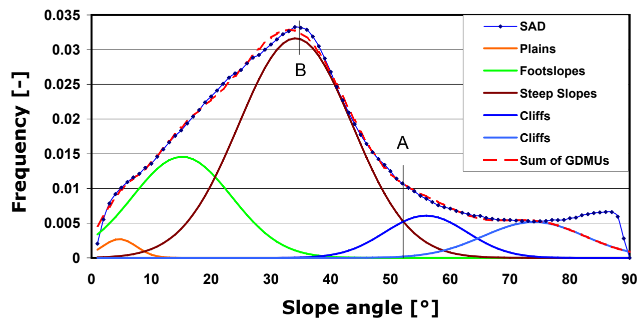

Fig. 3. Slope angle distribution (SAD) of 1° bin size from *Les Diablerets* Alpine Valley test zone featuring the GDMU of the topography. This test site is entirely situated in the Helvetic HMA. A indicates the threshold slope angle above which the slopes belong dominantly to the cliffs and are therefore considered as potential rockfall source area. B indicates the mode of the GDMU steep slopes. The two cliffs units represent two families of bare rock cliff faces lithologically distinct (for explanations refer to Sect. 2.3).

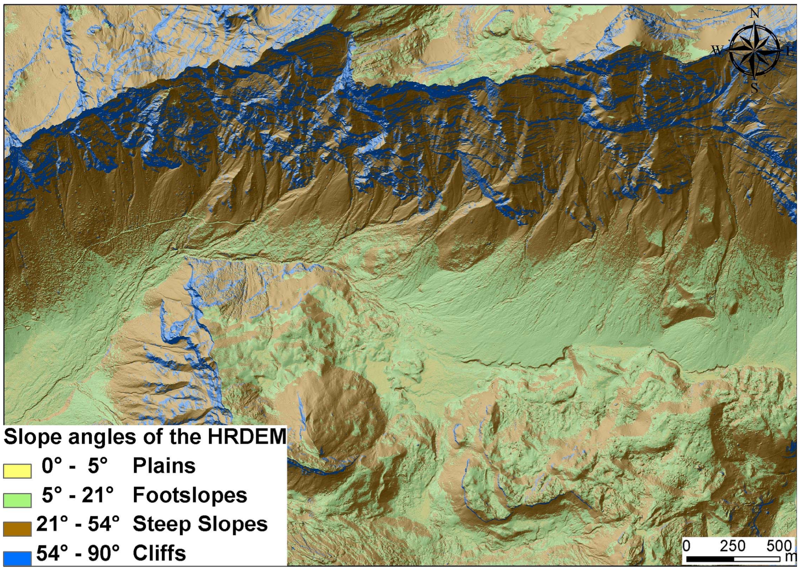

Fig. 4. Hillshade of *Les Diablerets* region displaying with distinct colours the dominant MU extracted from the intersections between GDMU plotted in Fig. 3. Comparison shows that GDMU are accurately superimposed with the morphological units observed on the hillshade (MNT-MO, © 2005 SIT).

2.3 GDMU interpretations

Each Gaussian slope angle distribution can be considered as typical of landscape. The mode of the distribution can be assumed as the average apparent slope angle of stability of a given MU. Consequently in a given landscape, the slope angle of a MU varies around an average as this is for instance the case for scree slopes, which possess an average slope angle close to 35°. As an example, the SAD of the two undisturbed scree deposits illustrated in Fig. 5 accepts the Kolmogorov-Smirnov test (p-value >0.05 and KS-STAT > CV) performed over the SAD sample [31.5°–39.5°]. This means that the slope angle values come from a standard normal distribution. For each HMA, the decomposition of the SAD in GDMU can be interpreted as follow (Fig. 3):

1. A threshold slope angle is defined at the intersection (noted A) between the two steepest MU: the GDMU cliffs and the GDMU steep slopes (Rouiller et al., 1998). All DEM cells with slopes steeper than this threshold angle are considered as potential rockfall source areas, independently of the local lithology and the land cover, because they are cliffs or rocky slope surfaces lightly covered with vegetation.

2. In some cases, there are no GDMU cliffs within the decomposition of the SAD. Thus, the highest GDMU is referred to the rocky steep slopes MU.

3. In very steep topography the SAD can contain two GDMU cliffs. In that case the lower GDMU cliffs is considered and used to estimate the above threshold (1).

4. In the present study the 1:25 000 Swiss topographic vector map (©Swisstopo: DV012716) was used, which contains geo-thematic information among others the cliff outcrops as polygons. However, they can display slope angles down to 0° where rockfall are very unlikely. As a consequence, only the cliff outcrops areas with slope angle value above the mode of the GDMU steep slopes (noted B) are assumed to be potential rockfall sources.

Finally, all these criterions were used to identify potential rockfall source areas within a standard GIS environment for each considered HMA.

3 Data processing

The present study was performed over the entire Canton of Vaud (Switzerland) that represents an area of about 3200 km^2. The method was applied using HRDEM of 1 m cell size (MNT-MO, ©2005 SIT). The results were compared and analysed using orthophotos by inspecting talus screes and blocks deposits over the entire study area. Field observations were performed in specific test zones of each HMA in order to evaluate the quality of the model.

3.1 Homogeneous morphometric areas (HMA)

The Canton of Vaud consists of three main tectonic units (Trümpy, 1980; Escher et al., 1997): the Jura, the Prealps and the Swiss Molasse Plateau (Fig. 6). The western part, the Jura Mountains, is formed by a folded and thrusted Mesozoic to Tertiary carbonates platform series, in a thin skin

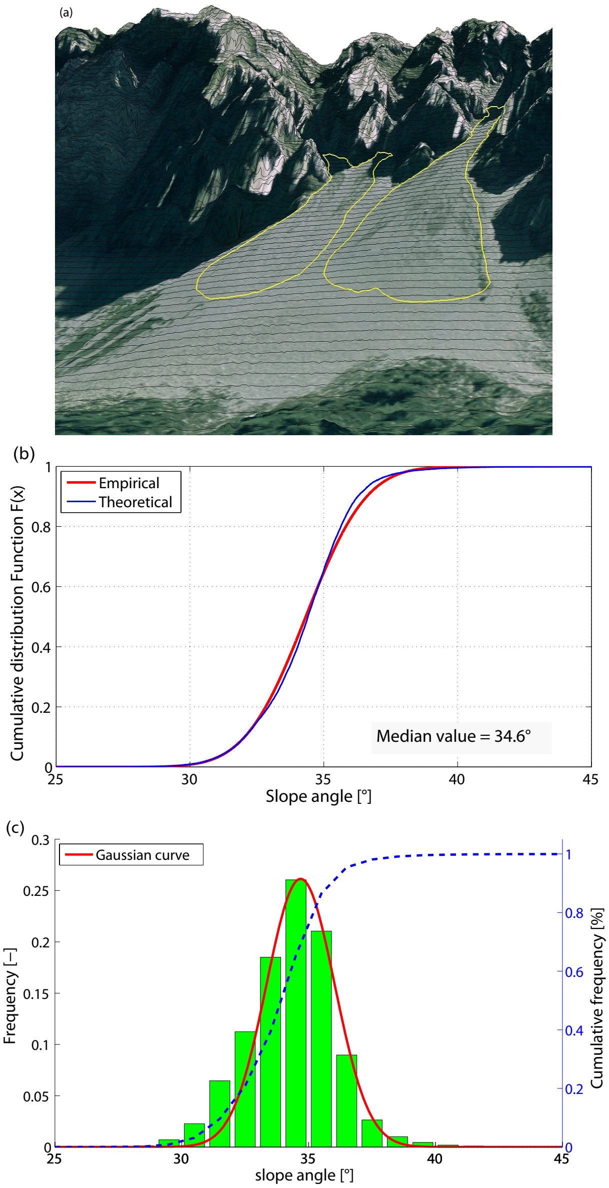

Fig. 5. (a) Scree slopes at Mt D'Or, near *Les Diablerets* region. The undisturbed scree deposits are delineated in yellow. **(b)** Scree deposits CDF of the slope angles. Results of the Kolmogorov-Smirnov test statistic: p-value = 0.0679, CV = 0.056 and KSSTAT = 0.058. **(c)** SAD of the two scree deposits with its mode = 34.5°.

tectonic style. The elevation of the Jura mountain chain ranges between 400 m a.s.l. to 1700 m a.s.l. The southeast part of the study area belongs to the Alps. They inherited a glacial landscape, which was reworked by fluvial erosion processes and mass movements. Its rugged topography range from 400 m a.s.l. to more than 3000 m a.s.l. The main lithologies are limestones, dolomites, marls, evaporites and shales, which were deposited in several different Mesozoic and Cenozoic basins. Those lithologies control strongly the

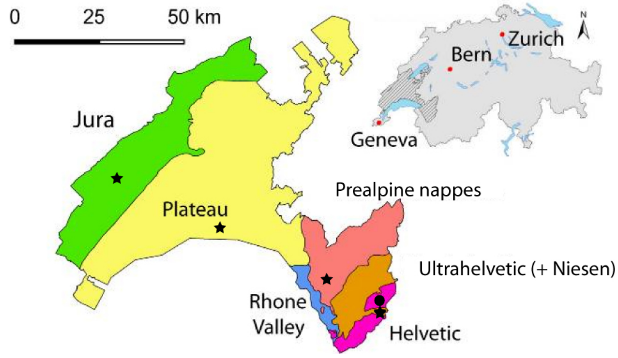

Fig. 6. Geographical location of the Canton of Vaud (Switzerland) with the main HMA. The black dot indicates the test site location of *Les Diablerets* and the black stars the test site of the other HMA.

type of slope movements. This area is divided in three main structural units: the Prealpine nappes deriving mainly from the Briançonnais domain, the Helvetic nappes and the Ultrahelvetic nappes (including the Niesen nappe). Between the Jura and the Alps lies the molassic Plateau. This is a sedimentary foreland basin formed in Oligocene to Miocene, during the Alpine orogeny. Its topography is mostly flat with small hills. The rocks are mainly terrigeneous sediments deposited in marine or continental environments.

3.2 Processing HRDEM and SAD analysis

The HRDEM was processed within the GIS environment ArcGIS®. The SAD analysis is obtained from standard DEM slope angle computation (Burrough and McDonnell, 1997). The slope angles are computed using a 3×3 matrix (Horn, 1981) implemented in the ArcGIS® spatial analyst extension and corrected according to Eq. (1). The slope angle β was classified in bins size of 1°. Five distinct HMA were defined based on the above structural units: Helvetic, Ultrahelvetic (+Niesen) and Prealpine nappes belonging to the Alps, the Plateau and Jura. For the three HMA of the Alps, the SAD was modelled integrally over the considered area. For the Jura and the Plateau, however, the slope angles were computed according to 30 cross-sections evenly distributed along the rugged areas only, as described in Sect. 2.2.

The SAD decomposition in GDMU was performed using the Solver of Excel (©Microsoft) to perform the minimization. Initial parameters that are set manually are the number of GDMU, their estimated mean slope value and standard deviation. These initial values were defined according to the shape of the SAD, where some changes along the curvature of the distribution can be observed. Each GDMU was compared with observations on the hillshade of the HRDEM, orthophotos and the geological and topographical maps. If required, the process started over again with new initial values to increase the matching with the observed morphology. This approach is summarized in the Fig. 7.

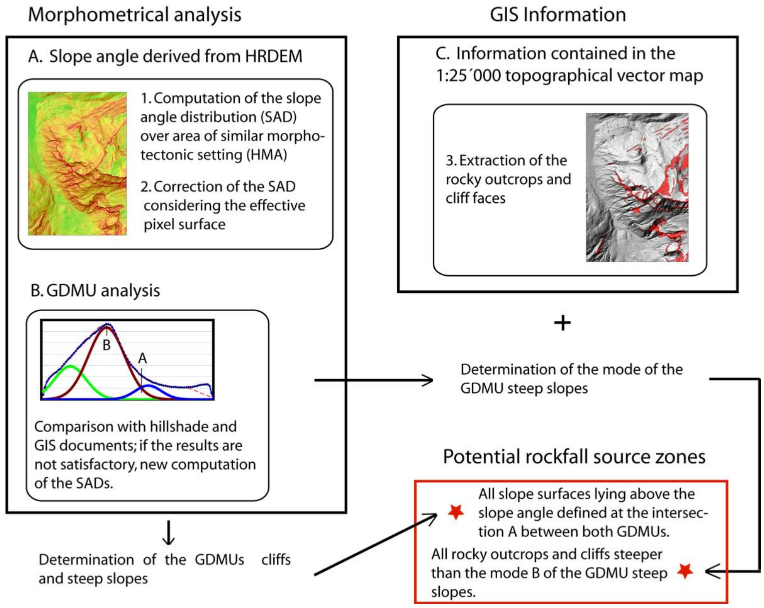

Fig. 7. Flow chart describing the methodology.

4 Results

The threshold slope angles resulting from the computation of the SAD and the extraction of their relative GDMU were interpreted separately for each HMA. The results are analysed according to their specific geology and morphology respectively, since their SAD are strongly influenced by the dominant lithologies. Threshold values obtained for each HMA are summarized in Table 1 and the map of potential rockfall source zones for the entire Canton of Vaud is shown in Fig. 11.

4.1 Alpine HMA

In the three Alpine HMA, the decomposition of the SAD into four GDMU can be clearly achieved (Fig. 8). The sum of these Gaussian distributions reproduces the SAD with a coefficient of determination close to 1, meaning that the morphologies can be described by the SAD decomposition. The analysis of the hillshade derived from HRDEM and the orthophotos show that the modelled cliffs are delineated accurately. The comparison of the results with field observations and the geological maps show that the modelled potential rockfall sources are mainly located in the limestone and dolomites. In these HMA, the lower slope angle intersection of the GDMU cliffs seems to depend on the percentage of limestone and dolomites per HMA outcropping: the Helvetic containing the greatest area, the Ultrahelvetic (+Niesen) the lowest and the Prealpine nappes in between. These lithologies are very competent and form in great majority the very steep slopes and cliffs. Hence, the morphometric analysis

Table 1. Threshold slope angles above which rockfall source areas are potentially considered.

Location	HMA	Threshold angles for: A. Slopes belonging to the GDMU cliffs	Threshold angles for: B. Cliffs and rocky outcrops taken from the topographic vector map (mode of the GDMU steep slopes)
Alps	Helvetic	54°	36°
	Préalpes Médianes	53°	34°
	Ultrahelvetic	49°	33°
Plateau	Molassic Plateau	46°	30°
Jura	Jura Mountains	46°	32°

performed in the Alpine units seems to extract the geological constraints as well.

According to SAD analysis, the threshold slope angle for the cliffs ranges in the Alps between 49° for the Ultrahelvetic to 54° for the Helvetic, with an angle of 53° for the Prealpine nappes (Table 1). This simply underlines the fact that Ultrahelvetic nappes are mostly composed of flysch-type deposits creating rock outcrops with lower slope angles than the carbonates belonging to the Helvetic and Prealpine nappes. In addition, it is interesting to notice that most of the mode values of the GDMU steep slopes are close to 35°, the slope angle of sand pile.

The illustration in Fig. 12 shows how all potentially unstable cliffs and rock slopes contained in the 1:25 000 topographic vector map are well constrained by the cliffs modelled with the GDMU approach. In Fig. 13,

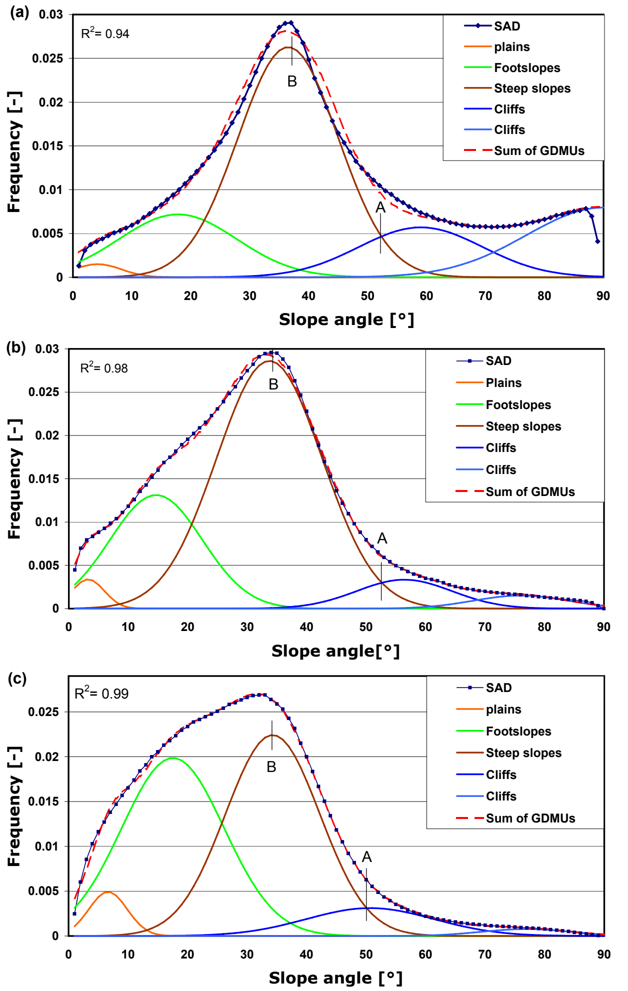

Fig. 8. Results of the SAD decomposition for the Alpine HMA (**(a)** Helvetic HMA, **(b)** Préalpes Médianes HMA, and **(c)** Ultrahelvetic HMA). The numerical values are given in Table 1.

comparison with orthophotos analysis and field observations shows that including all cliffs and rocky outcrops contained in the Swiss topographical vector map steeper than this angle of stability improves the delineation of potential rockfall source zones.

4.2 Molasse Plateau HMA

In the contrary of the Alps, the Plateau was shaped differently. Its morphology results mainly from glacial and fluvial erosion processes. In this hilly topography with large flat terrain, the MU of the cliffs is lacking, even though small cliff faces can be encountered in some parts, but they are seldom. The methodology was then adapted and slope angle profiles were used. According to its specific geomorphological environment, the SAD was decomposed into three

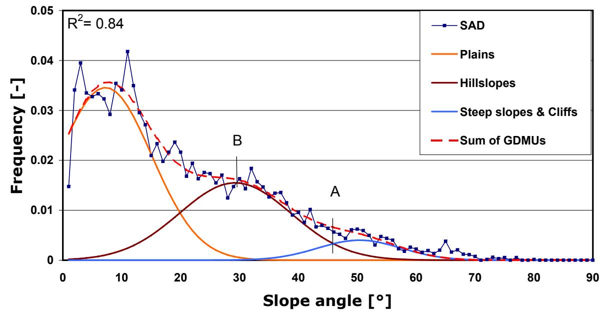

Fig. 9. Results of the SAD analysis for the HMA of the Plateau. According to its morphological environment, the SAD was decomposed into three GDMU only (see text for details). The numerical values are given in Table 1.

GDMU (Fig. 9):

1. The plains corresponding to the large flat terrain or areas of low steepness.

2. The hillslopes corresponding to the sides of the small hills.

3. Steep slopes and cliffs corresponding to areas of rugged topography.

The three GDMU could reproduce the SAD in an accurate way. The slope angle intersection of the GDMU steep slopes and cliffs with the GDMU hillslopes is modelled at 46°. And the mode of the GDMU hillslope is at 30°. By analysing orthophotos and shaded reliefs, the modelled potential rockfall source areas show that steep rocky slopes arise predominantly along rivers and impermanent watercourses, as well as at the limits of fluvio-glacial terraces. These small cliffs resulting from fluvial erosion are made of marls and competent sandstones. Comparison with orthophotos analysis and field observations is very satisfactory and allows considering the modelled slopes as potential rockfall source areas.

4.3 Jura Mountains HMA

Although the morphology is different than in the Alps, four main GDMU were used. The Jura morphology is constrained by a thin skin tectonic style. Plains are situated in the synforms and gentle slope angles correspond to the box folds. Erosion of folds limbs and faults create cliffs in the limestone and marls and scree deposits corresponding to the steep slopes. The sum of the GDMU reproduces the SAD accurately (Fig. 10). The GDMU cliffs become dominant upon the GDMU steep slopes above a slope angle of 46°. The mode of the GDMU steep slopes yields to 32°. The analysis of the results with the hillshade shows that the potential rockfall source areas follow the steep parts of the folds where limestone outcrop on the surface or are covered under a thin layer of soil, or they correspond to some very steep slopes

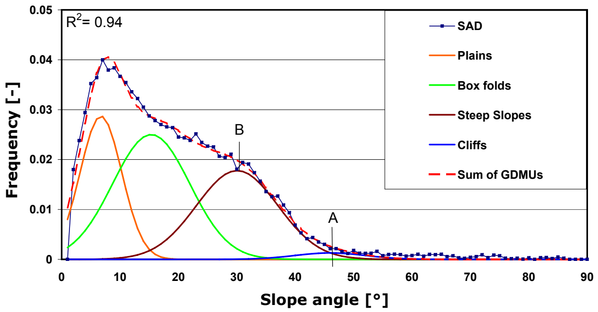

Fig. 10. Results of the SAD analysis for the HMA of the Jura. The numerical values are given in Table 1.

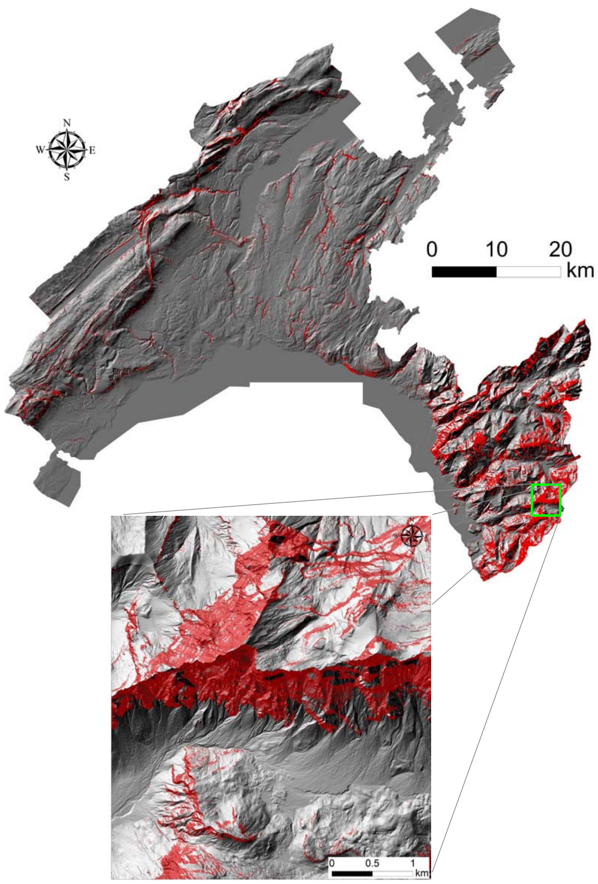

Fig. 11. Potential rockfall sources (in red) map for the entire Canton of Vaud with an original resolution at 1 m reduced 25 m cell size. The enlargement shows *Les Diablerets* test area (MNT-MO, ©2005 SIT).

formed by strike-slip faults (Trümpy, 1980). Historical registers of event and scree deposits observed on orthophotos show that rockfall sources are mostly encountered in those zones. By including all rocky outcrops of the topographic map steeper than the mode of the GDMU Steep slopes (32°), potential rockfall source areas coming from fluvial erosion could also be delineated.

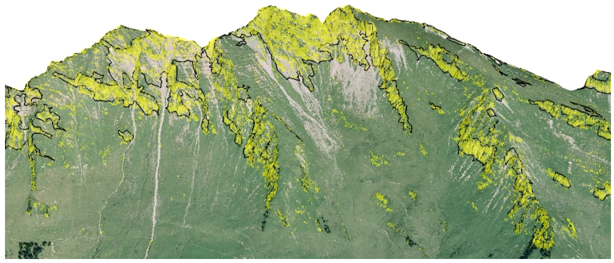

Fig. 12. Section of the test site situated in the Niesen nappe merged with Ultrahelvetic nappes, showing all slopes lying above the threshold slope angle of 49° (delineated in yellow). The cliffs and rocky outcrops taken from the Swiss topographical vector map are surrounded by a black line (SWISSIMAGE ©2004 swisstopo (DV012716)).

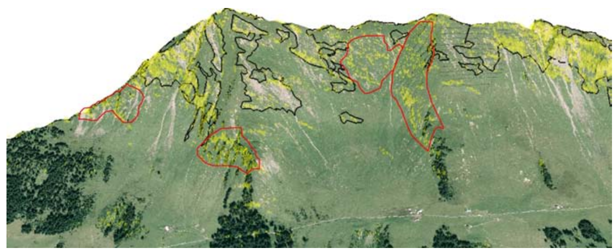

Fig. 13. Same test site as Fig. 12. All slopes lying above the threshold slope angle of 49° are delineated in yellow. The surrounding red lines show the additional rocky slopes detected by the SAD decomposition. This corresponds to the modelled cliffs zones that are not contained in the topographical vector map. Those areas lie above recent talus scree or freshly detached blocks and can therefore be described as potential rockfall sources. Such zones, sometimes lightly covered with vegetation, are not obviously included in hazard assessment (SWISSIMAGE ©2004 swisstopo (DV012716)).

5 Influence of the DEM resolution

According to the resolution of the DEM and the vertical size of the terrain elements, the SAD can vary as described in Fig. 2. The SAD analysis was thus performed on DEMs of *Les Diablerets* test zones with lower resolutions in order to study the changes in slope angle distribution of the four main MU. The SAD decompositions in GDMU were computed for each SAD according to their own initial parameters (e.g. Fig. 14). Then, the mode value of the GDMU steep slopes and the intersection of the GDMU cliffs with the GDMU steep slopes were compared between DEMs of 1 m to 25 m cell size, with a 5 m resolution step. Coarser DEMs were generated from the fine 1 m HRDEM using standard GIS tools, except for the 25 m that is a standard Swiss DEM (©Swisstopo (DV08371)).

The slope angle intersection value between the GDMU cliffs and steep slopes and its distribution mode show a progressive linear decrease when increasing the cell size of the DEM (Fig. 15). Notice that the linear decrease is more important for the intersection of the GDMU than for the mode

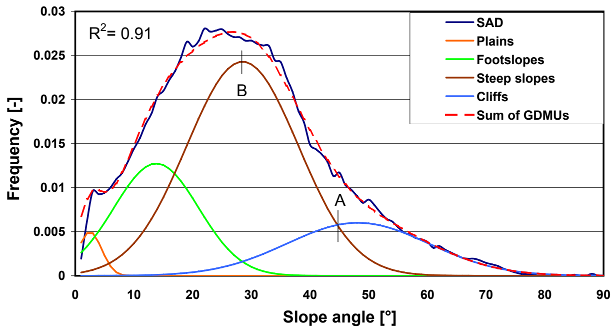

Fig. 14. SAD of *Les Diablerets* test site (same spatial extent as Fig. 3) decomposed using the standard Swiss DEM of 25 m cell size resolution. Note the decrease of the threshold slope angles (A = 45°; mode B = 28°) resulting from the smoothing effect of the coarser DEM resolution in comparison with the HRDEM thresholds angles of the Fig. 3.

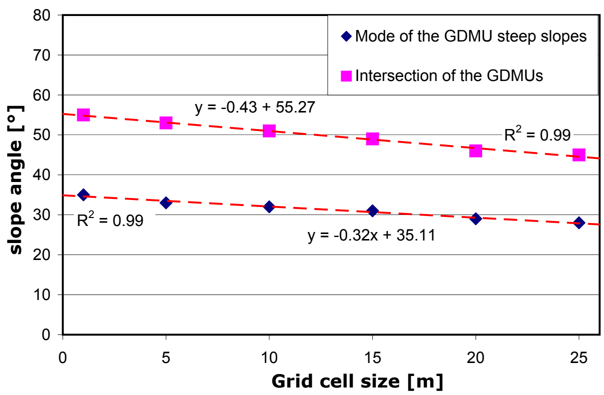

Fig. 15. Results of the SAD analysis performed over input DEM of 6 different resolutions on *Les Diablerets* test site.

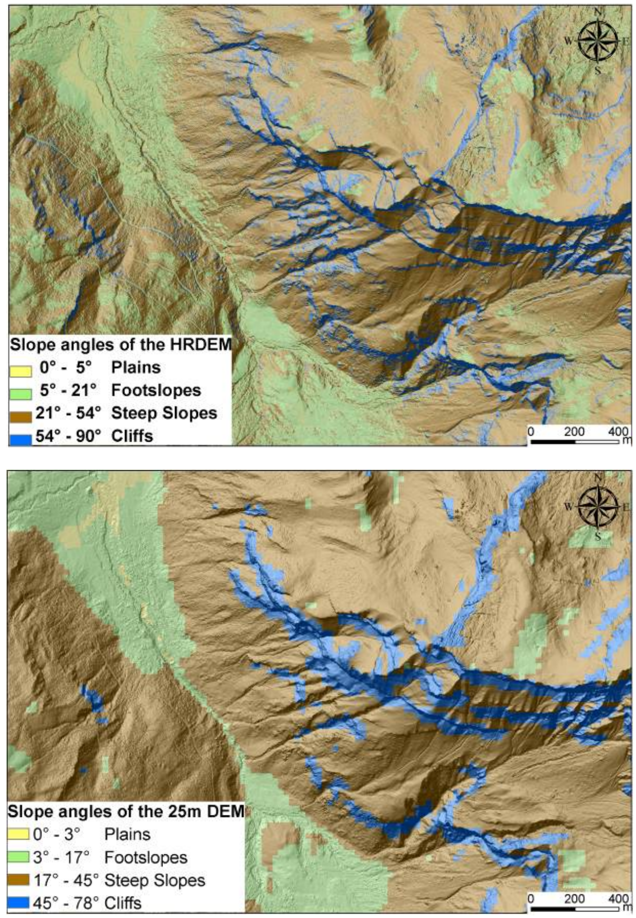

Fig. 16. Display of the main MU according to the SAD analysis performed on a DEM of 1 m and 25 m cell size (see Figs. 3 and 14) (MNT-MO, ©2005 SIT).

of GDMU steep slopes. Observation of the HRDEM shows that cliff faces above a certain size can be delineated (Fig. 2). The comparison displayed in Fig. 16 for instance shows that the cliffs are much more roughly delimited with the 25 m DEM, but surround well the ones detected by the present methodology performed on the HRDEM. In the case where cliffs or steep slopes are too small however, they are not constrained by the model. In the contrary, MU (e.g. footslopes) lying below a certain slope angle are only slightly influenced by the enhanced accuracy of the HRDEM. This analysis shows that even though the computed slope angle of coarser DEM resolution is an approximation, steep zones can be correctly extracted from DEM with large cell size using the SAD decomposition. Threshold slope angles are thus lower and therefore less in accordance with the "reality". Nevertheless, a majority of cliffs above a certain size are detected (Fig. 16), where potential rockfall source areas can be located. This can be used as an indicative overview for large scale rockfall hazard assessment. In addition, HRDEM highlights the small cliff faces and steep slopes from which a rockfall might initiate.

6 Conclusions

The present method based on slope angles statistics describes a systematic global approach to identify potential rockfall initiation areas at a regional scale. This is a rather conservative way to consider cliff faces and slope surfaces steeper than a threshold slope angle to be potentially unstable. The results show that estimated potential rockfall source zones correspond well to field observation performed on test zones and extracted from orthophotos analysis. The present study demonstrates that the SAD analysis works on rugged landscapes like in the Alps. This is due to the fact that major distinctive variations of the relief can be reflected more predominantly in the SAD decomposition. The SAD decomposition is very accurate for HMA with an important slope angle variation, like in the glacial-shape valley of the Alps. However, it can be applied elsewhere when considering the inhomogeneity of the topography. For large flat areas or hilly topography, the computation of the Gaussian curves is more ambiguous due to the low frequency difference in steep slopes. This can be adjusted to the GDMU method by taking into account the zones where the topography is only rugged, using series of cross-sections. Comparisons with known rockfall events give evidences that it is possible to assess potential rockfall sources over large areas from DEM-based slope angle parameters, topographical elements and geological maps.

One of the great advantages of this approach is that it detects potential rockfall source zones located on steep slopes covered with vegetation as well, which are not often taken into account in rockfall source detection (Fig. 13).

Such detection of potential rockfall source areas can provide a fast and cost-effective overview of rockfall prone locations, without considering the structural setting in details. The method is not limited to HRDEM. For a general overview of potential rockfall initiation zones, this approach works with poorer resolution DEM as well. However, the contribution of HRDEM, like airborne laser scanning DEMs, is especially significant in detecting small-sized rock faces and steep slopes. This should be taken into account in the development of susceptibility or hazard maps at a regional scale. Outcomes could be used as groundwork for territory management and as overview to focus on detailed field investigations.

Acknowledgements. The authors would like to thank the authorities of the state of Vaud that supported financially this project and particularly D. Morratel and P. Fouvy for their collaboration. Moreover, they are grateful to M.-H. Derron from the Geological Survey of Norway (NGU) for his precious comments all along the development of this project. They appreciated the help of T. Oppikofer and C. Longchamp during the composition of this paper.

Edited by: K. Schellenberg
Reviewed by: J. Corominas and H. Seijmonsbergen

References

Aksoy, H. and Ercanoglu, M.: Determination of the rockfall source in an urban settlement area by using a rule-based fuzzy evaluation, Nat. Hazards Earth Syst. Sci., 6, 941–954, 2006, http://www.nat-hazards-earth-syst-sci.net/6/941/2006/.

Acosta, E., Agliardi, F., Crosta, G. B., and Rìos Aragués, S.: Regional Rockfall Hazard Assessment in the Benasque Valley (Central Pyrenees) using 3D numerical Approach, Tech. rep., Project DAMOCLES, 2007.

Baillifard, F., Jaboyedoff, M., and Sartori, M.: Rockfall hazard mapping along a mountainous road in Switzerland using a GIS-based parameter rating approach, Nat. Hazards Earth Syst. Sci., 3, 435–442, 2003, http://www.nat-hazards-earth-syst-sci.net/3/435/2003/.

Baillifard, F., Jaboyedoff, M., Rouiller, J. D., Couture, R., Locat, J., Robichaud, G., and Gamel, G.: Towards a GIS-based hazard assessment along the Quebec City Promontory, Quebec, Canada, in: Landslides Evaluation and stabilization, edited by: Lacerda, W., Ehrlich, M., Fontoura, A., and Sayaõ, A. A., Balkema, 207–213, 2004.

Bunce, C. M., Cruden, D. M., and Morgenstern, N. R.: Assessment of the hazard from rock fall on a highway, Can. Geotech. J., 34, 344–356, 1997.

Burrough, P. and McDonnell, R. A.: Principles of Geographical Information Systems, Oxford University, 330 pp., 1997.

Crosta, G. B. and Agliardi, F.: A methodology for physically based rockfall hazard assessment, Nat. Hazards Earth Syst. Sci., 3, 407–422, 2003, http://www.nat-hazards-earth-syst-sci.net/3/407/2003/.

Derron, M.-H., Jaboyedoff, M., and Blikra, L. H.: Preliminary assessment of rockslide and rockfall hazards using a DEM (Oppstadhornet, Norway), Nat. Hazards Earth Syst. Sci., 5, 285–292, 2005, http://www.nat-hazards-earth-syst-sci.net/5/285/2005/.

Escher, A., Hunziker, J. C., Marthaler, M., Masson, H., Sartori, M., and Steck, A.: Geological framework and structural evolution of the Western Swiss-Italian Alps. Deep structure of Switzerland – Results of NFP-20, Birkhäuser Basel, 205–222, 1997.

Frattini, P., Crosta, G., Carrara, A., and Agliardi, F.: Assessment of rockfall susceptibility by integrating statistical and physically-based approaches, Geomorphology, 94, 419–437, 2008.

Gokceoglu, C., Sonmez, H., and Ercanoglu, M.: Discontinuity controlled probabilistic slope failure risk maps of the Altindag (settlement) region in Turkey, Eng. Geol., 55(4), 277–296, 2000.

Günther, A.: SLOPEMAP: programs for automated mapping of geometrical and kinematical properties of hard rock hill slopes, Comput. Geosci., 29(7), 865–875, 2003.

Günther, A., Carstensen, A., and Pohl, W.: Automated sliding susceptibility mapping of rock slopes, Nat. Hazards Earth Syst. Sci., 4, 95–102, 2004, http://www.nat-hazards-earth-syst-sci.net/4/95/2004/.

Guzzetti, F., Carrara, A., Cardinali, M., and Reichenbach, P.: Landslide hazard evaluation: a review of current techniques and their application in a multi-scale study, Central Italy, Geomorphology, 31, 181–216, 1999.

Guzzetti, F., Crosta, G., Detti, R., and Agliardi, F.: STONE: a computer program for the three-dimensional simulation of rock-falls, Comput. Geosci., 28(9), 1079–1093, 2002.

Guzzetti, F., Reichenbach, P., and Wieczorek, G. F.: Rockfall hazard and risk assessment in the Yosemite Valley, California, USA, Nat. Hazards Earth Syst. Sci., 3, 491–503, 2003, http://www.nat-hazards-earth-syst-sci.net/3/491/2003/.

Hantz, D., Vengeon, J. M., and Dussauge-Peisser, C.: An historical, geomechanical and probabilistic approach to rock-fall hazard assessment, Nat. Hazards Earth Syst. Sci., 3, 693–701, 2003, http://www.nat-hazards-earth-syst-sci.net/3/693/2003/.

Heim, A.: Bergsturz und Menschenleben, Fretz and Wasmuth Verlag, Zurich, 218 pp., 1932.

Hoek, E. and Bray, J. W.: Rock Slope Engineering, in: The Institution of Mining and Metallurgy, London, 3rd edn., 358 pp., 1981.

Horn, B. K. P.: Hill shading and the reflectance map, Proceedings of the IEEE, 69(1), 14–47, 1981.

Jaboyedoff, M. and Labiouse, V.: Preliminary assessment of rockfall hazard based on GIS data, in: 10th International Congress on Rock Mechanics ISRM 2003 – Technology roadmap for rock mechanics, South African Institute of Mining and Metallurgy, Johannesburgh, South Africa, 575–578, 2003.

Jaboyedoff, M., Baillifard, F., Couture, R., Locat, J., and Locat, P.: New insight of geomorphology and landslide prone area detection using DEM, in: Landslides: Evaluation and Stabilization, edited by: Lacerda, W., Ehrlich, M., Fontoura, A., and Sayaõ, A., Taylor & Francis, London, 191–198, 2004a.

Jaboyedoff, M., Baillifard, F., Couture, R., Locat, J., and Locat, P.: Toward preliminary hazard assessment using DEM topographic analysis and simple mechanic modeling, in: Landslides: Evaluation and Stabilization, edited by: Lacerda, W., Ehrlich, M., Fontoura, A., and Sayaõ, A., Taylor & Francis, London, 199–205, 2004b.

Jaboyedoff, M., Baillifard, F., Derron, M.-H., Couture, R., Locat, J., and Locat, P.: Switzerland Modular and evolving rock slope hazard assessment methods, in: Landslide and avalanches, edited by: Senneset, K., Flaate, K., and Larsen, J. A., ICFL, 187–194, 2005a.

Jaboyedoff, M., Dudt, J. P., and Labiouse, V.: An attempt to refine rockfall hazard zoning based on the kinetic energy, frequency and fragmentation degree, Nat. Hazards Earth Syst. Sci., 5, 621–632, 2005b, http://www.nat-hazards-earth-syst-sci.net/5/621/2005/.

Jaboyedoff, M., Metzger, R., Oppikofer, T., Couture, R., Derron, M.-H., Locat, J., and Turmel, D.: New insight techniques to analyze rock-slope relief using DEM and 3D-imaging cloud points: COLTOP-3D, Rock mechanics Vol. 1: Meetings Society's Challenges and demands, chap. 7, 61–68, edited by: Eberhardt, E., Stead, D., and Morrison, T., 2007.

Krummenacher, B.: Modellierung der Wirkungsräume von Erd- und Felsbewegungen mit Hilfe Geographischer Informationssysteme (GIS), Schweizerischen Zeitschrift für Forstwesen, 146, 741–761, 1995.

Leroi, E., Bonnard, C., Fell, R., and Mc Innes, R.: State of the art paper: Risk assessment and management, in: Landslide risk management, edited by: Hungr, O., Fell R., Couture, R., and Eberhardt, E., Balkema, 59–198, 2005.

Locat, J., Leroueil, S., and Picarelli, L.: Some Considerations on the Role of Geological History on Slope Stability and the estimation of the Minimum Apparent Cohesion of a Rock Mass, in: Landslides, in research, theory and practice, edited by: Bromhead, E., Dixon, N., and Ibsen, M.-L., Thomas Telford, London, 2000.

Marquinez, J., Menéndez Duarte, R., Farias, P., and Juménez Sánchez, M.: Predictive GIS-based Model of Rockfall Activity in Mountain Cliffs, Nat. Hazards, 30, 341–360, 2003.

Mazzoccola, D. F. and Hudson, J. A.: A comprehensive method of rock mass characterization for indicating natural slope instability, Q. J. Eng. Geol. Hydroge., 29(1), 37–56, 1996.

Meissl, G.: Modellierung der Reichweite von Felsstürzen. Fallbeispiele zur GIS-gestützten Gefahrenbeurteilung aus dem Beierischen und Tiroler Alpenraum, Innsbrucker geografischen studien 28, Ph.D. thesis, Universität Innsbruck, 1998.

Montgomery, D. R. and Brandon, M. T.: Topographic controls on erosion rates in tectonically active mountain ranges, Earth Planet. Sc. Lett., 201(3–4), 481–489, 2002.

Rouiller, J. D., Jaboyedoff, M., Marro, C., Philippossian, F., and Mamin, M.: Pentes instables dans le Pennique valaisan. Matterock: une méthodologie d'auscultation des falaises et de détection des éboulements majeurs potentiels, Rapport final du PNR31, VDF Hochschulverlag AG, ETH Zürich, Switzerland, 1998.

Selby, M. J.: Hillslope Materials and Processes, 2nd edn., Oxford University Press, 1993.

Strahler, A. N.: Equilibrium theory of erosional slopes approached by frequency distribution analysis, Am. J. Sci., 248, 673–696, 800–814, 1950

Strahler, A. N.: Quantitative geomorphology of erosional landscapes, Compt. Rend, 19th Intern. Geol. Cong., Sec. 13, 341–354, 1954.

Toppe, R.: Terrain models – a tool for natural hazard mapping, IAHS, 162, 629–638, 1987.

Trümpy, R.: Geology of Switzerland, a Guide Book, Part A. An outline of the geology of Switzerland, Wepf & CO., Basel, Switzerland, 1980.

van Dijke, J. J. and van Westen, C. J.: Rockfall hazard, a geomorphological application of neighbourhood analysis with ILWIS, ITC – Publication Number, 1, 40–44, 1990.

Varnes, D. J.: Slope movements: types and processes, in: Landslide analysis and control, Transportation Research Board, Special Report 176, edited by: Schuster, R. L. and Krizek, R. J., Washington, DC, 11–33, 1978.

Wagner, A., Oliver, R., and Leite, E.: Rock and debris slide risk maps applied to low-volume roads in Nepal, Transportation Research Record 1106. TRB, National Research Council, Washington, DC, 255–267, 1988.

Whalley, W. B.: Rockfalls, in: Slope Instability, edited by: Brunsden, D. and Prior, D. B., Wiley, Chichester, 217–256, 1984.